SIMULATION OF HORIZONTAL AND VERTICAL THERMAL GRADIENT IN PETROLEUM RESERVOIR

Pablo Julián Rodriguez
DEP-FEM-UNCAMP-Cx.P.6122 Campinas, SP 13083-970
pablo@dep.fem.unicamp.br

Anibal Rubén Maldonado
DEP-FEM-UNCAMP-Cx.P.6122 Campinas, SP 13083-970
anibal@dep.fem.unicamp.br

Antônio Cláudio de França Correa
DEP-FEM-UNCAMP-Cx.P.6122 Campinas, SP 13083-970
acfcorrea@petrobras.com.br

***Abstract**: This work was developed with the goal of improving a numerical simulation model before production, seeking a better thermodynamic and phenomenological characterization of the reservoir, implementing a fully implicit method in a compositional simulator, using finite-difference discretization method to solve the material balance. To deal with nonlinear and sparse systems of equations caused by the fully implicit method, the Newton method was introduced to control convergence. Another important concept introduced into the mathematical model, not considered by other authors, is the molecular diffusive flux that is linked to the material balance. The simulation model consists of a two-dimensional reservoir, simplified in its petrophysical properties; in the first case the reservoir fluids are a ternary mixture and in the second case a real oil. The algorithm of resolution has proceeded by the assumption that the reservoir can be approximated by an initial condition of a pseudo-transient state with a homogenous composition reservoir that reaches a steady state in the thermodynamic equilibrium. As a result, two-dimensional maps of density and composition were generated.*

***Keywords**: compositional simulator, finite difference, thermodynamic characterization.*

1. Introduction

In this particular line of research, one-dimensional reservoir models were solved by Schulte (1980), who characterized qualitatively the Vertical Compositional Gradient (GCV) using a Cubic State Equation (EOS). According to Montel and Gouel (1985), the thermal effect can be as relevant as gravitational effects. According to Wheaton (1991), a 20% margin of error in the oil in-place estimation could be made when the GCV is not taken into account.

All of the works mentioned above follow the one dimensional approach of the compositional segregation phenomena. This issue was boarded with a two-dimensional reservoir model by Jacqmin (1990) considering free convection originated by the geothermal and horizontal thermal gradients. Later, Riley and Firoozabadi (1998) presented the first work that considers natural convection and diffusion in binary mixtures at reservoir conditions. Then, Ghorayeb and Firoozabadi (1999) showed a more embraced work about the compositional variation in multi-component mixtures, considering free convection and molecular diffusion in a porous media for hydrocarbon reservoirs; therefore, this last work was chosen as a basic model for this work.

The generic reservoir under study in this paper, located near a marine slope, shows a vertical geothermal gradient and a horizontal gradient due to the fact that one of the borders is closer to the marine slope as shown in Figure 1. The temperature in the bottom of the sea is constant and equal to 4°C. This two-dimensional thermal gradient causes a natural convection flux inside the reservoir, generating segregation of the mixture through the porous media. Those features show an important existence of compositional gradients. This compositional variation is widely observed in many reservoirs around the world and it has a strong effect over the characterization of reservoir/fluid, such as: viscosity, density, volume in-place and even development of immiscibility in porous media.

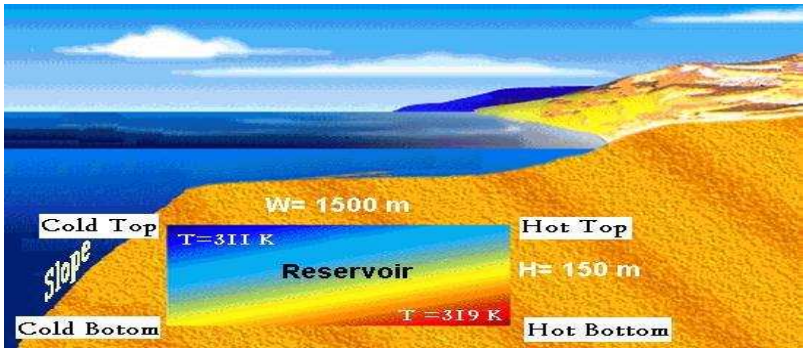

Figure 1: Geometry and temperature conditions of the reservoir near marine slope.

For this purpose, a two-dimensional and homogeneous compositional model was built to characterize a “clean” reservoir (before beginning of production).

2. Description of the model

The relevant features of the two-dimensional reservoir model used were: width=1500 m, height=150 m, porosity=0.25, reference temperature (middle of the reservoir)=315K, vertical thermal gradient=3.5K/100 m, horizontal thermal gradient=1.5K/1000 m, reference pressure (middle of the reservoir)= $7x10^6$ Pa, permeability: 0-1000 mD.

Two mixtures were used in this work:

- ideal ternary mixture (25% methane, 25% ethane, 50% butane),
- multicomponent (C1 to C31+) real oil mixture.

The temperature and pressure conditions were held the same to compare the real simulation and the ideal mixture, the wide range of permeability variations were used to determine this effect in compositional segregation.

The number of components of the real oil was reduced to a “pseudo ternary mixture”: heavier, medium, lighter; this process required a thermodynamic state equation to determine the pseudo component properties. The thermodynamic properties are presented in Tab. 1 and Tab. 2.

Table 1: Real oil thermodynamic properties after calculation of the three pseudo components properties using a Equation of State Peng-Robinson (EOS-PR).

	molar fraction	$\overline{M}$ [Kg/Kmol]	Tc[K]	Pc [Pa]	Vc[m^3/Kmol]	Tb[K]	Ac
LP	0.345	26.4	263.2	$46x10^6$	133.5	204.3	0.058
MP	0.452	132.7	615.6	$25x10^6$	512	440.7	0.430
HP	0.203	308.6	810.7	$13x10^6$	1116	647.5	0.890

where LP, MP, HP, $\overline{M}$, Tc, Pc, Vc, Tb and Ac are lighter, medium and heavier pseudo-components, molecular mass, critical temperature, critical pressure, critical volume, Boyle temperature and acentric factor of each pseudo-component respectively.

Table 2: Thermodynamic properties for both mixtures and the molar diffusion coefficient estimated by algorithm of Firoozabadi (1999).

	ρ $\left[\frac{Kg}{m^3}\right]$	μ [cP]	β_T $\left[\frac{1}{K}\right]$	β_{X1}	β_{X2}	D_{11} $\left[\frac{m^2}{s}\right]$	D_{12} $\left[\frac{m^2}{s}\right]$	D_{21} $\left[\frac{m^2}{s}\right]$	D_{22} $\left[\frac{m^2}{s}\right]$	D_1^P $\left[\frac{m^2}{Pa.s}\right]$	D_2^P $\left[\frac{m^2}{Pa.s}\right]$	D^T $\left[\frac{m^2}{K.s}\right]$	D_2^T $\left[\frac{m^2}{K.s}\right]$
TM	450	0,067	0,052	-1,25	-0,72	$3,1.10^{-9}$	$-0,8.10^{-9}$	$-0,3.10^{-9}$	$4,7.10^{-9}$	$0,3.10^{-16}$	$0,1.10^{-11}$	5.10^{-11}	2.10^{-11}
RO	752	0,046	-8.10^{-4}	2.10^{-3}	6.10^{-4}	$4,7.10^{-9}$	$-2,8.10^{-9}$	$-3,8.10^{-9}$	$3.3.10^{-9}$	$0,2.10^{-16}$	$1,6.10^{-16}$	1.10^{-11}	1.10^{-11}

where TM, RO, ρ, μ, β_T, β_{xi}, D_{ij}^M, D_i^P, D_i^T are ternary mixture, real oil, density, viscosity, thermal and molar expansion coefficients, molar, pressure and thermal diffusion of components respectively.

The following hypotheses were adopted in the development of the model: pore compressibility is neglected, permeability is uniform and constant for each case, viscosity depends on T,P and composition, homogenous system, the flow of oil components is slow compared with the stabilization time of the pseudo transient state, the reservoir has sealing faults in the lateral, top and bottom boundaries (no flux through those boundaries), approximation of the mixture of hydrocarbons by three pseudo components, the temperature could be considered constant because the heat capacity of porous media is sufficiently larger than that of the hydrocarbon mixture, the bottom hole pressure is known (Initial Condition).

2.1. Mathematic model:

A two-dimensional porous medium was considered with width *b* and height *h*, saturated by a single-phase mixture of *n* components.

The unsteady-state conservation equations of mass and species are:

$$\frac{\partial c}{\partial t} + \nabla.(c.v) = 0 \tag{1}$$

$$\frac{\partial (c.x_i)}{\partial t} + \nabla.(c.x_i.v) + \nabla.J_i = 0 \quad \text{i=1,2...n-1} \tag{2}$$

where: c,v, and J_i are the total molar density, velocity and diffusive molar flux for the component **i** respectively.

We assume that the Oberbeck-Boussinesq approximation is valid. In this approximation, the density is assumed to be constant, except in the buoyancy term ($\rho g \boldsymbol{z}$), where it varies linearly with the temperature and the mole fractions.

$$\rho = \rho_0 \left[1 - \beta_T (T - T_0) - \sum_{i=1}^{n-1} (\beta_x)_i (x_i - x_{i0}) \right] \tag{3}$$

where ρ is the mixture density, β_T and $(\beta_x)_i$ are the thermal and compositional expansion coefficient respectively for *d=1, 2*. By combining Eq. (1), Eq. (3) and Darcy's Law, Eq. (4) is obtained, allowing for the implicit calculation of the pressure in each point of the reservoir for three components:

$$\nabla^2 P = \rho_o.g.\left(\beta_T.T_Z + \beta_{X1} \frac{\partial x_1}{\partial z} + \beta_{X2} \frac{\partial x_2}{\partial z} \right) \tag{4}$$

where P, g are pressure and gravity acceleration respectively and introducing the concept of diffusive molar flux:

$$J_i = -c\left(\sum_{d=1}^{n-1} D_{i,d}^M.\nabla x_d + D_i^P.\nabla P + D_i^T.\nabla T \right) \tag{5}$$

where D_i^M, D_i^P and D_i^T are the molar, pressure and thermal coefficients respectively.

Once defined the thermodynamic properties of the pseudo components mixture, Eq. (2), Eq. (4) and Eq. (5) plus the Equation of State were incorporated to the algorithm to solve a two dimensional map of P, ρ and composition.

2.2. Features of the model (numerical model)

The strategy used to determine the variation of thermodynamic properties along the reservoir is described as: during the first time-step the reservoir is supposed to be homogeneous, although the system is not under thermodynamic equilibrium. In the next time-steps, diffusion and convection flux are generated seeking to achieve the thermodynamic equilibrium and generating compositional variation. Finally, the equilibrium condition is reached when the compositional variation in each block of the reservoir between two time-steps can be considered neglectable: $\left| (x_i(y,z))^{t+\Delta t} - (x_i(y,z))^t \right| \le \delta;\ \forall y \in [0, L] \wedge z \in [0, H]$ where x_i, y, z, L, H, t are a generic component, the horizontal and vertical spatial dimensions, the width and height of the reservoir and the time dimension respectively. This condition is achieved when the sum of diffusive and convective flux is neglected for each block of the reservoir $\left\{ c.\nabla\left[(x_1)_{i,j}^k.(v)_{i,j}^k \right] + \nabla (J_1)_{i,j}^k \right\} \le \delta$ for *i=1,2,...n* , where "k" is the time-step when the convergence is reached.

2.3. Numerical scheme

Fully-implicit and semi-implicit schemes were used for the temporal integration to compare their results. This work seeks the steady-state solution and iterates on the unsteady state until the steady state is reached. In this work, convergence to the steady state is assumed when the absolute error of mole fractions is less than 10^{-7} between two successive iterations at each grid point. The grid size used was 9x13 with variable time-step.

Using a second-order centered scheme for the spatial discretization of Eq. (4), one obtains Eq.(6):

$$\nabla^2 P = \frac{P_{i-1,j} - 2P_{i,j} + P_{i+1,j}}{\Delta y^2} + \frac{P_{i,j-1} - 2P_{i,j} + P_{i,j+1}}{\Delta z^2} = \rho_o.g.\left(\beta_T.T_Z + \beta_{x1} \frac{\partial x_1}{\partial z} + \beta_{x2} \frac{\partial x_2}{\partial z} \right)_{ij} \tag{6}$$

By reorganizing the terms of the last equation and changing the sub index (**i,j**) to the MxN dimension vector **k**, as shown in Fig. (3A), Eq.(7) is obtained:

$$\Delta z^2 P_{k+1} + \Delta y^2 P_{k+N} + \Delta z^2 P_{k-1} + \Delta y^2 P_{k-N} - 2(\Delta y^2 + \Delta z^2) P_k$$
$$= \rho_o . g . \left(\beta_T . T_Z + \beta_{x1} \frac{(x_1)_{k+N} - (x_1)_k}{\Delta z} + \beta_{x2} \frac{(x_2)_{k+N} - (x_2)_k}{\Delta z} \right) . \Delta y^2 . \Delta z^2 \quad (7)$$

2.3.1. Initial conditions and contour condition

The initial condition is $P_i = P_0$ for all the blocks of the reservoir in the first time-step and the contour conditions required to represent a sealing reservoir are:

-*Dirichlet* condition: applied to fix a pressure value at the top and bottom of the reservoir.

-*Newman* condition: applied under the pressure derivate in the specific case of sealing reservoir and it represents a "mirror condition" at the laterals boundaries, as shown in Fig.(3B).

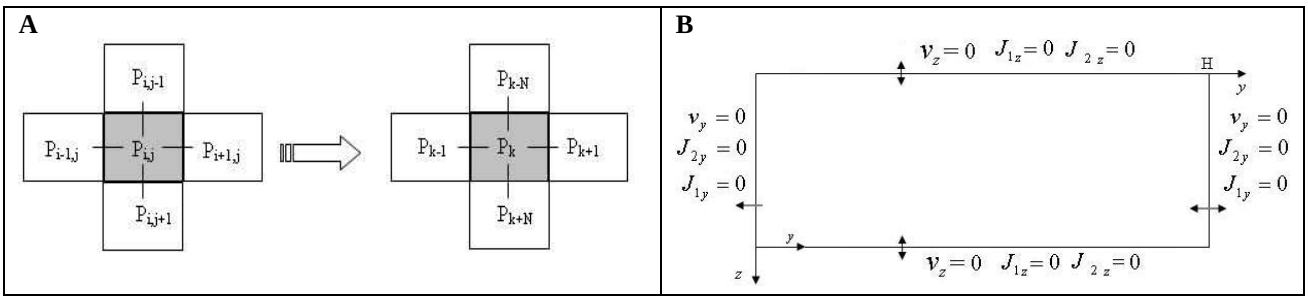

Figure 3: **A** represents the new one-dimensional sub index for the pressure and the other properties. **B** shows the Newman border condition of the reservoir

Upper boundary: $P_{k-N} = P_{k+N} - 2\Delta z.\rho.g$ - Lower boundary: $P_{k-N} = P_{k+N} + 2\Delta z.\rho.g$ -Lateral boundaries: $P_{k+1} = P_{k-1}$

Once contour conditions were applied, the in Eq. (5), the system of Eq. (7) is represented as a matricial resolution: $\overline{\overline{[A]}} * \overline{P} = \overline{B}$, where $\overline{P}$ is the MxN vector that represents the field pressure of each block , $\overline{B}$ is the independent terms vector that includes the gravitational term of the Newman contour condition from the top and from the bottom and $\overline{\overline{[A]}}$ is a $(MN)^2$ penta-diagonal matrix, whose components are:

$a_{i,i} = -2(\Delta y^2 + \Delta z^2)$: main diagonal coefficients,

$a_{i+1,i} = a_{i-1,i} = \Delta z^2$: beside upper and lower diagonal coefficients: those have lateral Newman contour condition,

$a_{i,i-N_y} = a_{i,i+N_y} = \Delta y^2$: far upper and lower diagonal coefficients: including the top and bottom Newman condition.

Where, in the Fig.(4), the trace line in the matrix **A** represents the Newman condition at the top and bottom in the far upper and lower diagonal coefficients respectively. The zeros and twos are the Newman contour condition at the right and left side of the reservoir.

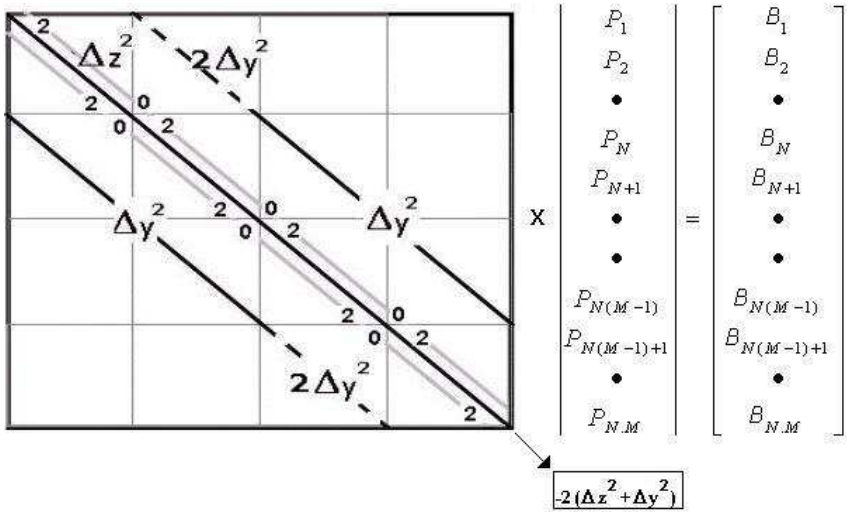

Figure 4: Representation of the penta-diagonal matrix system to solve the Pressure field, vector **P**.

Then, the resultant matricial system, which must to be solved with all the conditions (initial and contour) is:

$$\overline{P} = [A]^{-1}.\overline{B} \tag{8}$$

After the pressure in each cell of the grid is resolved, the Eq. (3) is used to determine the density field. The spatial discretization is performed by a centered scheme, wich estimates the diffusive flux from Eq. (5) and the velocity field from Darcy equation.

2.3.2. Explicit Method

Discretizing Eq. (2) by a 1st order discretization to solve the mathematical operator *Divergent:*

$$(x_i)_k^{t+1} = (x_i)_k^t - \Delta t.\left[\left(\frac{(v_y.x_i)_{k+1/2} - (v_y.x_i)_{k-1/2}}{\Delta y}\right)^t + \left(\frac{(v_z.x_i)_{k+N/2} - (v_z.x_i)_{k-N/2}}{\Delta z}\right)^t + \frac{1}{c}\left(\frac{(J_i)_{k+N/2} - (J_i)_{k-N/2}}{\Delta z}\right)^t + \frac{1}{c}\left(\frac{(J_i)_{k+1/2} - (J_i)_{k-1/2}}{\Delta \partial y}\right)_k^t\right] \tag{9}$$

In Eq. (9), the calculus of the molar composition in the next time-step is completely explicit.

At the left lateral boundary of the reservoir the discretization is replaced by the forward spatial discretization; however, in the right lateral boundary the backward spatial discretization should be used instead.

2.3.3. Implicit Method

In this case, there is a system of two equations to solve in each block. These equations depend on themselves and border block molar fraction, therefore, the system need to be solved simultaneously.

$$\frac{\partial x_i}{\partial t} + v_y\frac{\partial x_i}{\partial y} + v_z\frac{\partial x_i}{\partial z} - D_{i1}\left(\frac{\partial^2 x_1}{\partial y^2} + \frac{\partial^2 x_1}{\partial z^2}\right) - D_{i2}\left(\frac{\partial^2 x_2}{\partial y^2} + \frac{\partial^2 x_2}{\partial z^2}\right) - D_i^P.\rho_o.g\left(\beta_{x1}\frac{\partial x_1}{\partial z} - \beta_{x2}\frac{\partial x_2}{\partial z} - \beta_T.T\right) = \nabla\left(D_i^T.\nabla T\right) \tag{10}$$

for $i, j = 1,2$ and $j \neq i$

$$\overline{F} = d.\overline{x}_{j+N_y} + b.\overline{x}_{j+1} + e.\overline{x}_{j-N_y} + c.\overline{x}_{j-1} + a.\overline{x}_j - \overline{f} \tag{11}$$

The implicit system was resolved using the Multidimensional Newton method, and for this purpose the $\overline{F}$ Jacobian matrix is required:

$$Ja_j = \left[\begin{bmatrix} \frac{\partial F_1}{\partial x_{11}} & \frac{\partial F_1}{\partial x_{21}} \\ \frac{\partial F_2}{\partial x_{11}} & \frac{\partial F_2}{\partial x_{21}} \end{bmatrix} \begin{bmatrix} \frac{\partial F_1}{\partial x_{12}} & \frac{\partial F_1}{\partial x_{22}} \\ \frac{\partial F_2}{\partial x_{12}} & \frac{\partial F_2}{\partial x_{22}} \end{bmatrix} \cdots\cdots \begin{bmatrix} \frac{\partial F_1}{\partial x_{1j}} & \frac{\partial F_1}{\partial x_{2j}} \\ \frac{\partial F_2}{\partial x_{1j}} & \frac{\partial F_2}{\partial x_{2j}} \end{bmatrix} \cdots\cdots \begin{bmatrix} \frac{\partial F_1}{\partial x_{1MN}} & \frac{\partial F_1}{\partial x_{2MN}} \\ \frac{\partial F_2}{\partial x_{1MN}} & \frac{\partial F_2}{\partial x_{2MN}} \end{bmatrix}\right] \tag{12}$$

$$Ja.\delta\overline{x} = -\overline{F} \tag{13}$$

$$\delta\overline{x} = \overline{x^t} - \overline{x^{t+1}} \tag{14}$$

Eq. (14) estimates the composition of each component of the mixture in the next time-step. Once resolved the algorithm, Fig. (5) shows the flowchart of the complete iteration.

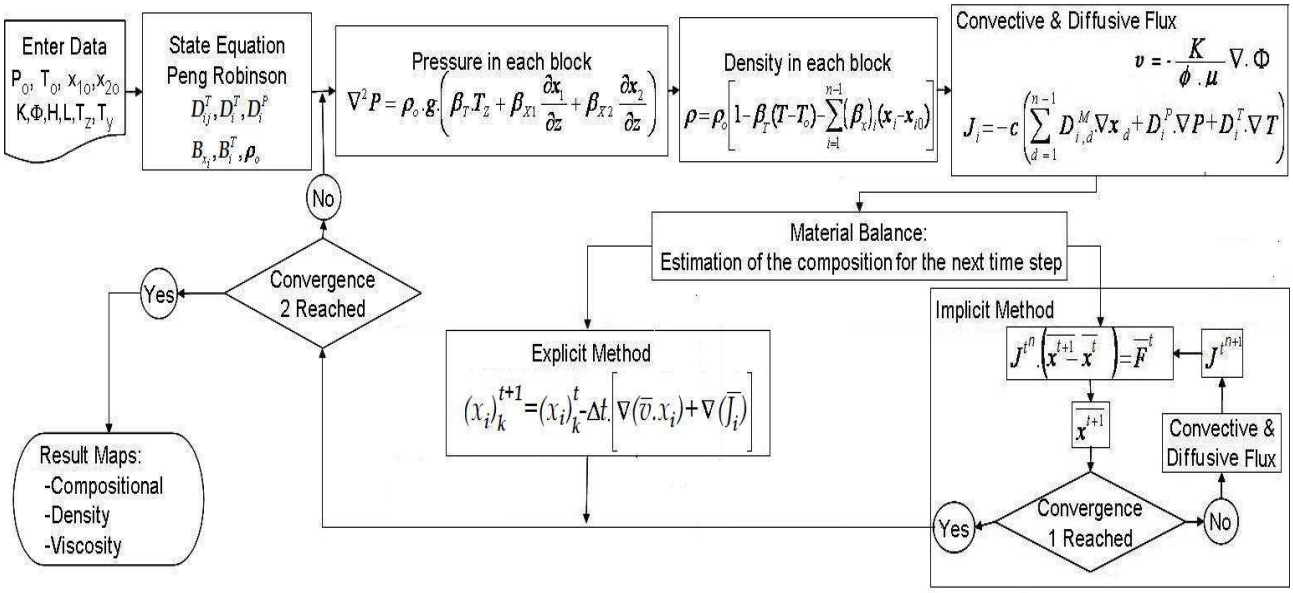

Figure 5: Algorithm flowchart of explicit and implicit method used in the thermodynamic simulation.

3. Results

First, the three-component mixture was simulated for a wide range of permeability values using either implicit or explicit method. Due to the near ideal behavior, both methods showed convergence and similar results; nevertheless, the explicit method was faster.

Simulations by fully implicit and semi implicit methods were compared for several reservoir permeabilities (from zero: pure diffusion to 1000 mD). The difference between both methods was more pronounced for the high permeability cases. In this case, the explicit method often could not reach a stable state and the result depended on the initial point, therefore, the method became unreliable. On the other hand, the fully implicit method achieved the convergence (the absolute error tended to zero) unconditionally and independent of the initial condition.

Figure 6 shows that for low permeabilities, in ternary mixtures methane segregates towards the bottom-hot side of the porous media. In this ternary mixture, the maps do not differ between fully implicit or semi implicit method at low or high permeability. The same behavior was observed when the result of the molar compositional maps was compared with the result obtained by Firozabadi (1999).

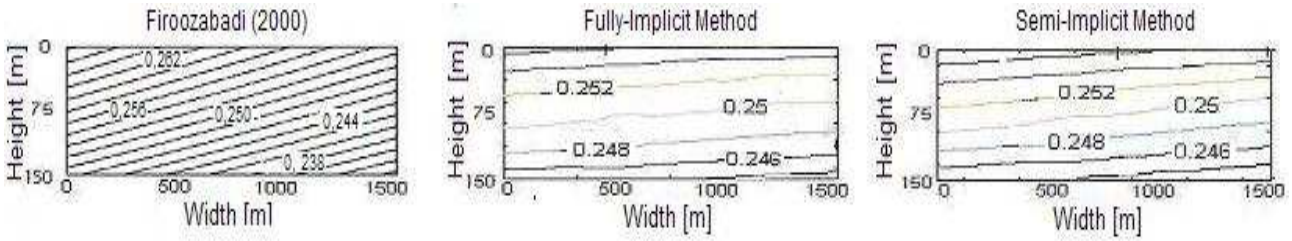

Figure 6: Methane composition obtained by Firoozabadi (1999), fully-implicit and semi-implicit method for a ternary mixture of hydrocarbons (methane-ethane-butane) and permeability 10 mD.

The separation factor is defined like a ratio between the concentration, of any component, at the top and at the bottom of the reservoir. This parameter illustrates the same trend in the simulation results when compared for a wide range of permeabilities with Firoozabadi´s work (1999), as illustrated bf Fig.(7).

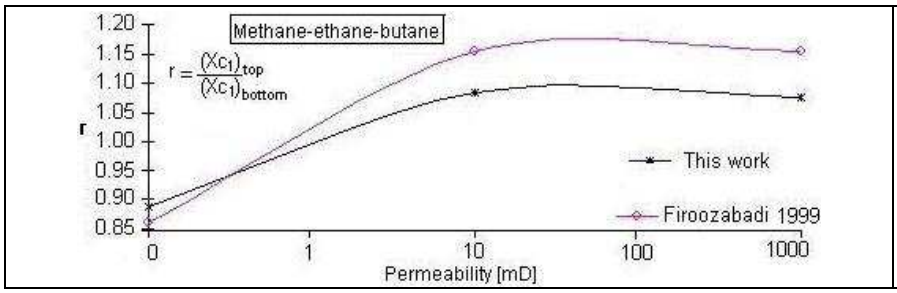

Number of iterations: Real Oil		
k [mD]	Explicit	Implicit
0	8340	15340
1	12470	17850
10	-----	19120
100	------	19120
1000	------	19120

Figure 7: Separation factor of methane obtained by Firoozabadi (1999) and in this work (left) and the number of iterations needed to achieve the stop condition when the implicit and explicit method are used.

The real oil case is shown in Fig. (8), for low permeabilities, the lighter pseudo component segregates towards the hot-top side of the porous media, unlike in ternary mixtures when it segregates to the cold-top. Despite that, both methods still present the same behavior for low permeabilities cases.

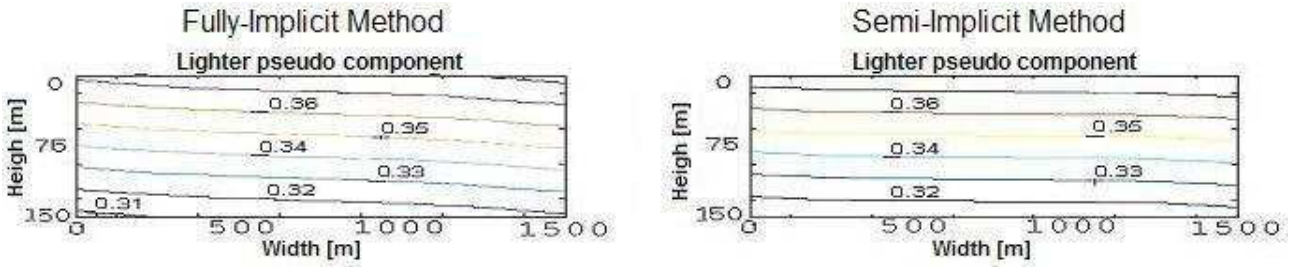

Figure 8: Lighter pseudo component molar fraction maps for real oil and permeability 1mD obtained by implicit resolution and explicit method.

The 3D surface in Fig. (9) shows the divergence between the fully implicit method and the semi implicit method in the molar compositional maps; whereas the lighter pseudo component segregates toward the cold-top of the reservoir in the fully implicit method; in the semi implicit method, the lighter pseudo component, segregates toward the hot-bottom and does not even show stability.

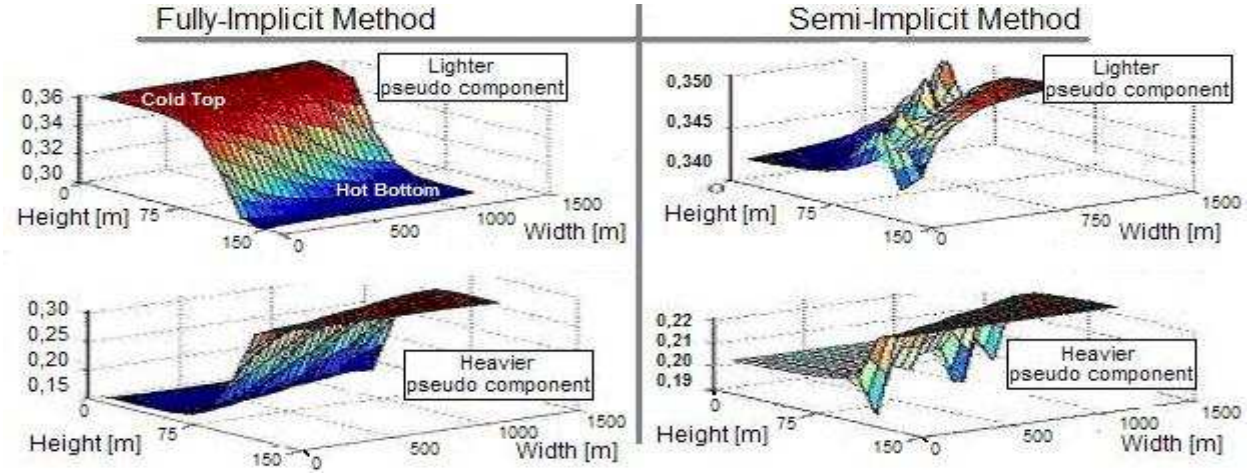

Figure 9: These maps represent the molar composition for real oil simulation, permeability 1000 mD, using fully-implicit and semi implicit method.

Another important observation to be made is: while at low permeabilities (1 mD) in Fig. (8), the lighter pseudo component segregates toward the hot-top of the reservoir, in the real oil example, the lighter pseudo component segregates to the cold-top of the reservoir when the permeability is increased (1000 mD), then the permeability plays an important role in the direction of segregation when different conditions of permeabilites are studied.

The 3D representation of the viscosity map in Fig. (10) has a similar shape than the heavier pseudo components in Fig. (9), thus demonstrating a close relationship between the composition with an important parameter of production

like viscosity. The density map in Fig. (10) depicts a weak dependence of this property with the molar segregation of the mixture, since the density has a stronger dependence with the thermal gradient

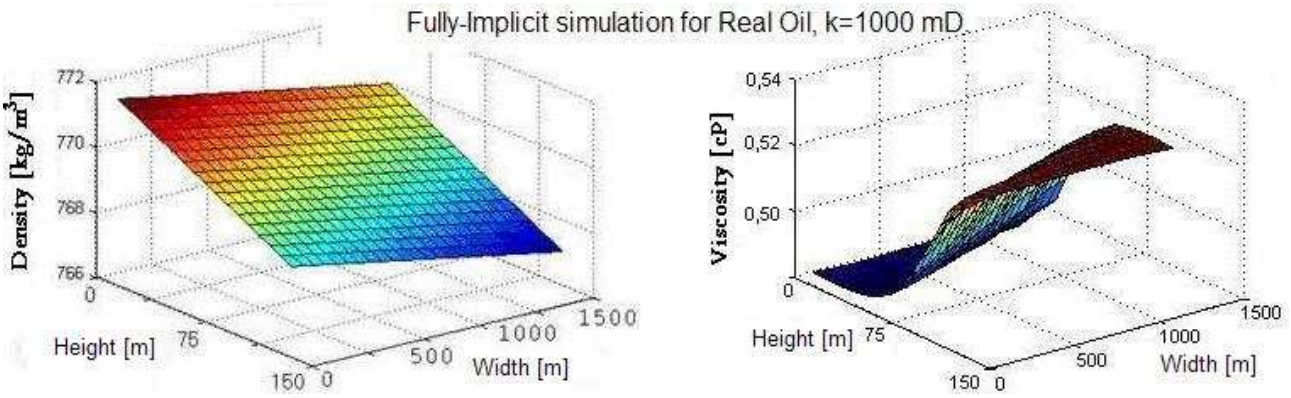

Figure 10: Real oil viscosity and density maps calculated by the fully implicit method.

The results for the real oil were more time consuming, increasing the number of simulations to achieve the steady state and the explicit method showed itself not to be completely reliable, especially when high permeability cases were simulated. This happens because, when the permeability increases, the convection flux starts to drive the direction of the molar flux inside the reservoir and compete against the diffusive flow, generating multidirectional flux that make the system not linear and more difficult to reach the convergence when the explicit method is used. On the other hand, the implicit method takes more time to achieve convergence, even thought, it is stable for all the cases simulated.

When a ternary mixture of hydrocarbon was studied, both reached the convergence, but when the mixture was a real oil (methane to $C31^{+}$), the Implicit Method was the only one that reached the convergence.

4. Conclusions

The effect of two dimensional segregation is only possible when a horizontal thermal gradient is present, that is, when the reservoir is near marine a slope. If the horizontal thermal gradient is not present, then the convective and diffusion effects will not exist; therefore, only the vertical segregation is possible.

Semi implicit integration is only possible adopting small time-step, however, in real oil case and high permeabilities, it can be unstable. The fully implicit method is unconditionally stable and the convergence of the algorithm does not depend of the initial point, although it formulation represents a bigger computational effort than the semi implicit method.

There are various features of compositional variation in hydrocarbon reservoirs depending on thermodynamic properties, molecular diffusion and natural convection. Those effects are not trivial, the orientation of the segregation varies with the P,T condition of the reservoir and even with the composition of the mixture.

5. References

Montel F.; Gouel P. L., 1985 “Prediction of Compositional Gradient in a Reservoir Fluid Column” SPE 14410.

Firozabaadi, A., 1999, *Thermodynamics of Hydrocarbon Reservoirs*. McGraw-Hill Publisher.

Ghorayeb, K., Firoozabadi, A., 1999, “Modeling Multicomponent Diffusion and Convection in Porous Media”, SPE Journal, pp. 158-171. *SPE* 62168.

Jacqmin, D., 1990, “Interaction of Natural Convection and Gravity Segregation in Oil/Gas Reservoirs”, SPE Reservoir Engineering, p. 233-238. *SPE 16703*.

Riley, M.; Firoozabadi A., 1998, “Compositional Variation in Hidrocarbon Reservoirs with Natural Convection and Difusion”, AIChE Journal, v.44, n.2, p.452-465.

Schulte, A. M., 1980, “Compositional Variations within a Hydrocarbon Column due to Gravity”, SPE Annual Technical Conference and Exhibition, Dallas, USA. *SPE* 9235.

Wheaton R., 1991, “Treatment of Variations of Composition with Depth in Gas-Condensate Reservoir”, SPE Reservoir Engineering, pp. 239-244. *SPE* 18267.

6. Responsibility notice

The authors are the only responsible for the printed material included in this paper.